Journal of the Ceramic Society of Japan 119 [9] 697-700 2011 Paper

Selective metallization of Ag_2O-dope silicate glass by femtosecond laser direct writing

Nan WU,† Xi WANG, Zhenxuan WANG, Masatoshi OHNISHI,*
Masayuki NISHI, Kiyotaka MIURA and Kazuyuki HIRAO

Department of Material Chemistry, Kyoto University Katsura, Nisikyo-ku, Kyoto 615–8510
***Qualtec Co., Ltd., 4–230 Sanbocho, Sakai-ku, Sakai, Osaka 590–0906**

We investigated the selective metallization on Ag_2O-doped silicate glass under femtosecond laser irradiation after electroless plating. We found, as increasing the laser power, the width of the ablated groove increased from 2.5 to 7.5 μm, and then the resulted new surface could offer an active site for reduction of Cu cations, leading to corresponding plated Cu lines with widths from 7.4 to 25.4 μm. The mechanism was supposed as irradiation of the femtosecond laser (FL) on Ag_2O doped silicate glass surfaces result in the reduction of silver ions, and consequently, then the formation of silver atoms or even silver nanoparticles became the seeds for the next electroless plating process.

Key-words : Femtosecond laser, Ag_2O-doped silicate glass, Multiphoton absorption

[Received June 10, 2011; Accepted July 12, 2011]

1. Introduction

In recent years, femtosecond laser microfabrication has received significant attention for its capability of making various functional microcomponents into a single substrate, so providing a new way to fabricate highly integrated microdevices such as lab-on-a-chips[1] and micro-total-analysis-system (μ-TAS) devices which allow chemical reactions and biomedical analysis to be performed within a small sample.[2)–4)] For example, μ-TAS is composed of some microfluidic components (such as micro-pumps, microvalves and micromixers) integrated by a glass chip with a size of the order from 1 to 10000 of mm^2. Based on μ-TAS, infusion, flow switching, particle separation, mixing, pumping, reaction of reagents and the analysis of reactants could be successively conducted. However, the electrical control of such a mechanical component by electromagnetic force is more desirable for accurate operation in μ-TAS applications. Thus, the development of a technique enabling the selective metallization on a glass substrate assumes even greater importance. One preparation strategy for μ-TAS devices is to use vacuum evaporation[5] or chemical vapor deposition (CVD)[6] to deposit metal thin films on a glass chip, but these methods are complicated and onerous in view of a needed resist process and vacuum for photolithography in micropatterning. Laser direct writing is expected to be an alternative method of forming patterns on metal thin films without photolithography. In this work, we report simple and convenient technique for selective metallization of Ag_2O-doped silicate glass by the FL direct writing with electroless copper plating.

2. Experimental

The experimental setup was in the following for making the silicate glasses of $70SiO_2 \cdot 10CaO \cdot 20Na_2O$ doped with Ag_2O (0.05 mol %). Reagent grade SiO_2, $CaCO_3$, Na_2CO_3, and Ag_2O were used as starting materials. Approximately 30 g batches were mixed and melted in platinum crucibles in an electronic furnace at 1600°C for 1 h under the ambient atmosphere. The melts were then quenched to room temperature to obtain transparent and colorless glasses. Ag_2O-doped glass was irradiated by using amplified FL pulses (250 kHz, 70 fs, 800 nm) of a mode-locked Ti-sapphire laser oscillator (Coherent; Mira and RegA). The FL pulses were attenuated by a neutral density filter and focused inside a soda lime glass plate (Schott B 270 Superwite) through a 20× objective lens (NA = 0.40; Nikon LU Plan ELWD 20). The glass sample was put on a computer-controlled XYZ stage, and the laser writing process was directly performed in air. Then, electroless copper (Cu) plating is carried out at room temperature for 20 min using a mixture of Cu-ion solution containing $CuSO_4$ 30 g/L, sodium potassium tartrate 100 g/L, NaOH 50 g/L, and formaldehyde 30 mL/L aqueous solution of formaldehyde (37.2 wt %). It is indispensable that the Ag_2O-doped silicate glass should be rinsed in deionized water after each step.

Using optical microscopy, we investigate the morphology of the Ag_2O-doped silicate glass sample. After the FL irradiation, the surface of the sample was analyzed by a X-ray photoelectron spectroscopy (XPS, ULVAC-PHI, Inc.). The exciting X-ray used for XPS was MgKα, 1254 ev, and 400 W. And the surface of electroless plating sample was analyzed by an electron probe micro-analyzer (EPMA, JEOL, JXA-8900-RL). All of the experiments were carried out at room temperature.

3. Results and discussion

The glass substrate was ablated at a laser power of 50–400 mW and a laser scanning speed of 50 μm/s. The resulted line widths of the groove are estimated to be about 2–8 μm. To verify the state of irradiation region, extinction spectrum and XPS was employed.

We measure absorption spectra in the wavelength range from 200 to 800 nm using a spectrophotometer before and after the focused irradiation of FL. Since the focal volume was too small to detect the absorption change using a spectrophotometer, we

† Corresponding author: N. Wu; E-mail: Wunan@collon1.kuic.kyoto-u.ac.jp

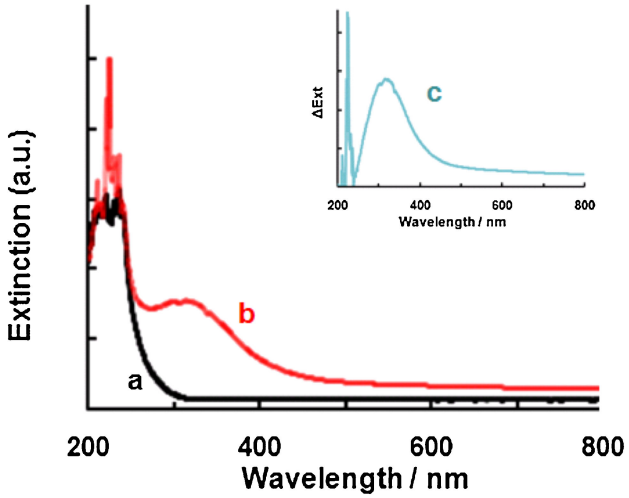

Fig. 1. (Color online) Extinction spectra of Ag_2O-doped glass (0.05 mol %) (a) before and (b) after FL irradiation. (c) Difference extinction spectrum of Ag_2O-doped glass (0.05 mol %) before and after the FL irradiation (inset of Figure).

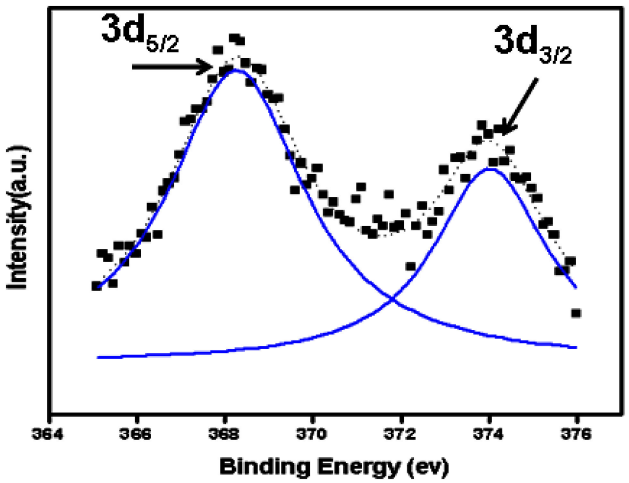

Fig. 2. (Color online) The XPS spectra of Ag 3d signals of the irradiated area in Ag_2O-doped glass. Blue curves are deconvolution results after fitting.

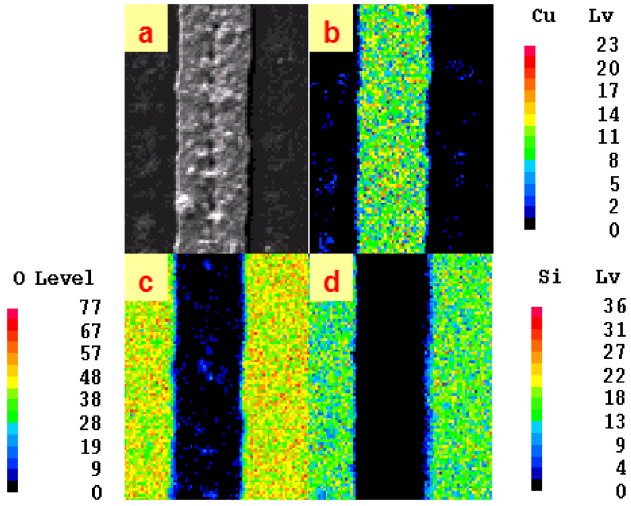

Fig. 3. (Color online) (a) FE-SEM images and EPMA images of (b) Cu, (c) O and (d) Si elements distribution after the irradiation. The laser power is 100 mW, and the laser scanning speed is set at 50 mm/s.

increased the irradiation area by scanning. Then we used scanning irradiation to produce irradiated lines in the surface of Ag_2O doped silicate glass by using a 20× objective lens (NA 0.40) and translating the samples perpendicular to the incident laser beam at a rate of 50 µm/s with a line period of 100 µm. The pulse energy was 200 mW. **Figure 1** shows the extinction spectra of the glass sample before (a) and after (b) the laser irradiation. No obvious absorption was observed for the non-irradiation glass sample in the wavelength region from 600 to 800 nm, while there was a significant absorbance from 200 to 600 nm wavelength in the irradiated region. The inset of Fig. 1, shows the difference in extinction spectrum of the Ag_2O-doped glass (0.05 mol %) before and after the FL irradiation. As demonstrated in Fig. 1(c), the extinction peaks of 230 and 330 nm can be assigned to the atomic silver and hole trap centers at non-bridging oxygen near Ag^+ ions, respectively.[8] Meanwhile, from the XPS images (**Fig. 2**) of the ablated Ag_2O-doped glass, we can assign Ag $3d_{5/2}$ and $3d_{3/2}$ to the binding energies of 368.2 and 374.2 eV, which exactly correspond to signals from atomic silver. All arguments are in good agreement with the preview data[7)–9)] and other published papers.[10)–14)]

Therefore, according to the above results of extinction spectrum and XPS, it can be concluded that the non-bridging oxygen should act as hole-trap centers while the Ag^+ ions as electron-trap ones. In that case, after irradiation by FL beam, an electron was driven out from the 2p orbital of a non-bridge oxygen in the SiO_4 polyhedron via the multiphoton absorption, while Ag^+ captured the electron to form an Ag atom. Consequently, the formation of silver atoms or even silver nanoparticles became the seeds for the subsequent electroless plating process.

Figure 3 shows FE-SEM images (a) and EPMA images (b, c and d) of as-ablated the Ag_2O-doped glass substrate after laser irradiation (power of 100 mW and scanning speed of 50 µm/s). The analysis of elements distribution in as-ablated area reveals that a large number of copper distributed in the middle of the area [Fig. 3(b)], while silicon and oxygen mainly distributed on both sides of the area [Figs. 3(c) and 3(d)]. In other words, straight lines of Cu thin film are selectively deposited along the glass substrate on the irradiated lines. Furthermore, we studied the dependences of the original ablated line-width and the followed plated Cu one on the laser power. As shown in **Fig. 4**, the line widths of the irradiated region and the plated Cu increase from 2.5 to 7.5 µm and from 7.4 to 25.4 µm, respectively, as the laser power increases. The broader line width of the Cu film than the line ablated before is likely to be the result of isotropic growth of the Cu film.

Figure 5 shows the optical micrographs (a, b) and EPMA images (c, d, e and f) of several cross sections of the copper microstructures, after the electroless plating process, which was deposited in the FL ablated grooves fabricated at a laser power of 100 mW (a, c and e) and 200 mW (b, d and f) with the same laser scanning speed of 50 µm/s. The distribution of Cu and Si elements are shown in Figs. 5(c) and 5(d), and Figs. 5(e) and 5(f), respectively. A large number of copper distributed in the middle of the area [Figs. 5(c) and 5(d)], while Silicon mainly distributed on both sides of the area [Figs. 5(e) and 5(f)]. The cross-sectional shapes of copper microstructures indicated that the Cu films are deposited only in the ablated grooves area but

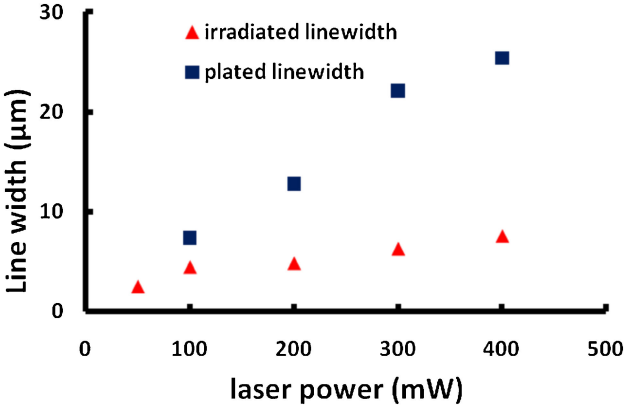

Fig. 4. (Color online) Dependences of irradiated and plated line widths on the laser powers.

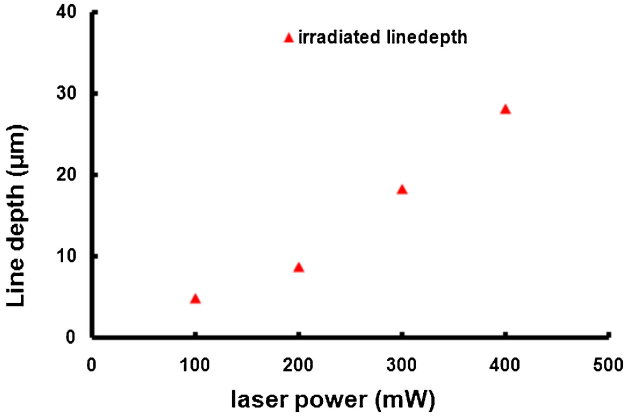

Fig. 6. (Color online) Dependences of irradiated line depths on the laser powers.

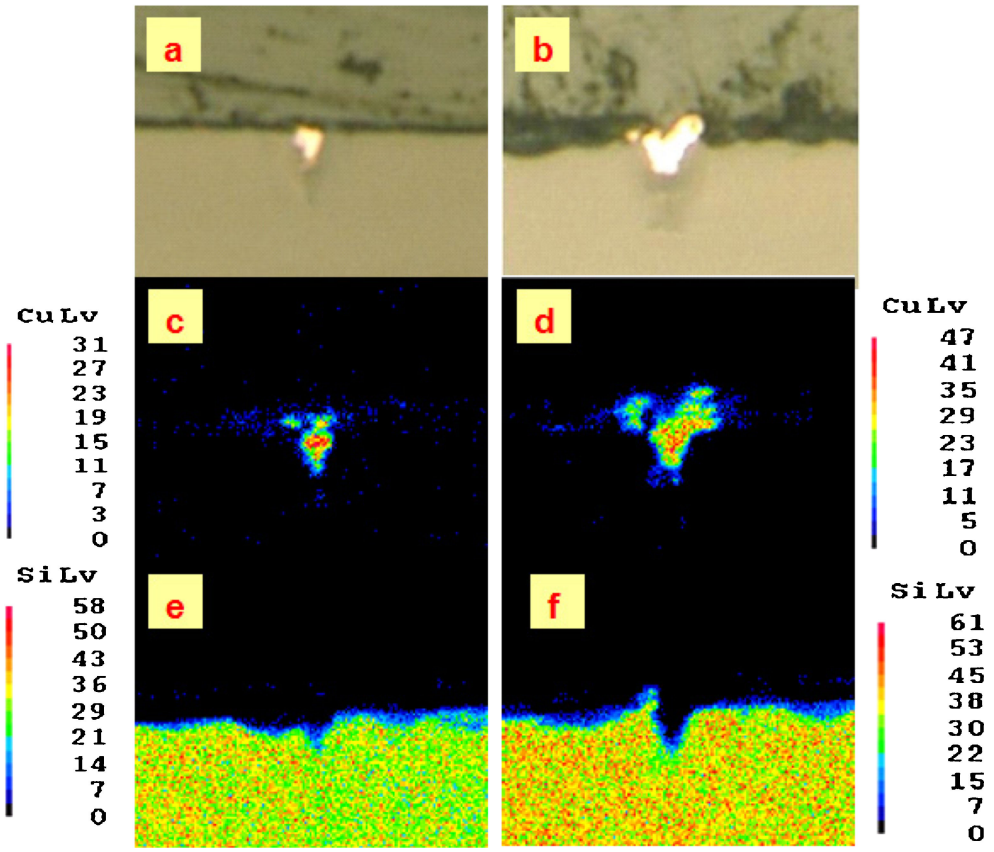

Fig. 5. (Color online) (a, b) Optical micrographs and (c, d, e and f) EPMA images of Cu and Si distribution on the cross sections of copper microstructures deposited inside the ablated grooves. The laser powers are100 mW (a, c and e) and 200 mW (b, d and f), and the laser scanning speed is set at 50 mm/s.

not on the non-irradiated surfaces at all, which indicates that the silver atoms are generated only on the groove surface under laser irradiation. Besides, the depth of laser ablated groove increased from 4.8 to 29 μm, shown in **Fig. 6**, with increasing the laser power. It is self-evident that the increase of groove depth will be beneficial for the fabrication of microelectrodes deeply embedded in transparent materials such as glasses or crystals.

From the above discussion, we deduced a possible of selective metallization (**Fig. 7**). When the FL beam is focused on the surface of the Ag_2O-doped glass, an electron was driven out from the 2p orbital of a non-bridging oxygen in the SiO_4 polyhedron via the multiphoton absorption only at the focused region. The Ag ions near the non-bridging oxygen captured the free electrons and were reduced to Ag atoms on the surface of Ag_2O-doped glass, as demonstrated in Fig. 7(a). Consequently, the formation of silver atoms or even silver nanoparticles became the seeds for the subsequent electroless plating process. In the electroless plating solution, only near the laser-irradiated regions, Cu atoms deposit and finally aggregate into Cu thin film [Fig. 7(b)].

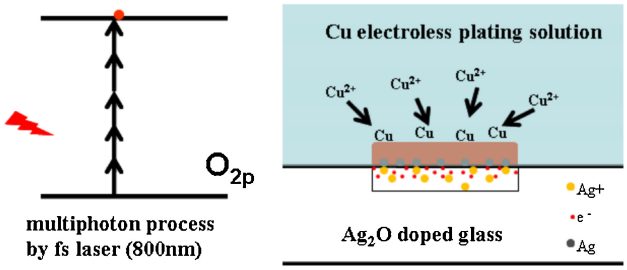

(a) (b)

Fig. 7. (Color online) (a) Generation mechanism of free electrons in glass by the FL for selective metallization. (b) Possible mechanism of the selective metallization of glass by electroless copper plating.

4. Conclusion

Due to the multiphoton reduction process, the reduction of an Ag ion to an atom by FL irradiation is essential in forming Ag nanoparticles, and the Ag atom acts as a crystal nucleus for copper growth. The copper thin film can be deposited only on the irradiation regions, when electroless Cu plating process is performed. We found that the line widths of the ablated region and the plated Cu increase from 2.5 to 7.5 µm and from 7.4 to 25.4 µm, the groove depths of the ablated region increase from 4.8 to 29 µm, respectively, as the laser power increases.

References

1) K. Sugioka, Y. Cheng and K. Midorikawa, *Appl. Phys. A: Mater. Sci. Process.*, 81, 1–10 (2005).
2) K. Hosokawa, M. Omata and M. Maeda, *Anal. Chem.*, 79, 6000–6004 (2007).
3) C. L. Bliss, J. N. McMullin and C. J. Backhouse, *Lab Chip*, 7, 1280–1287 (2007).
4) Y. Tanaka, K. Morishima, T. Shimizu, A. Kikuchi, M. Yamato, T. Okano and T. Kitamori, *Lab Chip*, 6, 362–368 (2006).
5) F. O. Lucas, A. Mitra, P. J. McNally, L. O'Reilly, S. Daniels, G. Natarajan, K. Durose, Y. Y. Proskuryakov and D. C. Cameron, *J. Mater. Sci. Mater. Electron.*, (online).
6) H. Liang and R. G. Gordon, *J. Mater. Sci.*, 42, 6388–6399 (2007).
7) J. Qiu, X. Jiang, C. Zhu, M. Shirai, J. Si, N. Jiang and K. Hirao, *Angew. Chem., Int. Ed.*, 43, 2230–2234 (2004).
8) M. Tashiro and N. Soga, *Kogyo Kagaku Zasshi*, 65, 342–346 (1962).
9) B. Hua, J. Qiu, Y. Shimotsuma, K. Fujita and K. Hirao, *J. Mater. Res.*, 20, 644–648 (2005).
10) T. Hongo, K. Sugioka, H. Niino, Y. Cheng and M. Masuda, *J. Appl. Phys.*, 97, 063517 (2005).
11) T. Baldacchini, A. C. Pons, J. Pons, C. N. LaFratta, J. T. Fourkas, Y. Sun and M. J. Naughton, *Opt. Express*, 13, 1275–1280 (2005).
12) T. Tanaka, A. Ishikawa and S. Kawata, *Appl. Phys. Lett.*, 88, 081107 (2006).
13) S. Maruo and T. Saeki, *Opt. Express*, 16, 1174–1179 (2008).
14) Y. Kondo, J. Qiu, T. Mitsuyu, K. Hirao and T. Yoko, *Jpn. J. Appl. Phys.*, 38, L1146–L1148 (1999).